the
abdus salam
international
centre
for theoretical
physics

united nations
educational, scientific
and cultural
organization

international atomic
energy agency

preprint

HARMONIC OSCILLATIONS, CHAOS AND SYNCHRONIZATION IN SYSTEMS CONSISTING OF VAN DER POL OSCILLATOR COUPLED TO A LINEAR OSCILLATOR

P. Woafo

31-09

IC/99/188

United Nations Educational Scientific and Cultural Organization
and
International Atomic Energy Agency
THE ABDUS SALAM INTERNATIONAL CENTRE FOR THEORETICAL PHYSICS

HARMONIC OSCILLATIONS, CHAOS AND SYNCHRONIZATION IN SYSTEMS CONSISTING OF VAN DER POL OSCILLATOR COUPLED TO A LINEAR OSCILLATOR

P. Woafo[1]
Laboratoire de Mécanique, Faculté des Sciences, Université de Yaoundé I, B.P. 812, Yaoundé, Cameroon
and
The Abdus Salam International Centre for Theoretical Physics, Trieste, Italy.

Abstract

This paper deals with the dynamics of a model describing systems consisting of the classical Van der Pol oscillator coupled gyroscopically to a linear oscillator. Both the forced and autonomous cases are considered. Harmonic response is investigated along with its stability boundaries. Condition for quenching phenomena in the autonomous case is derived. Neimark bifurcation is observed and it is found that our model shows period doubling and period-m sudden transitions to chaos. Synchronization of two and more systems in their chaotic regime is presented.

MIRAMARE - TRIESTE

December 1999

[1]Regular Associate of the Abdus Salam ICTP.

I- Introduction

Due to their occurrence in various scientific fields, ranging from biology, chemistry, physics to engineering, coupled nonlinear oscillators have been a subject of particular interest in recent years [1,2,3]. Among these coupled systems, a particular class is that containing self-sustained components such as the classical Van der Pol oscillator. The classical Van der Pol oscillator serves as a paradigm for smoothly oscillating limit cycle or relaxation oscillations [4]. In presence of an external sinusoidal excitation, it leads to various phenomena: harmonic, subharmonic and superharmonic frequency entrainment [5], devil's staircase in the behavior of the winding number [6], chaotic behavior in small range of control parameters [6-8]. The generalization of the classical Van der Pol oscillator to include cubic nonlinear term (the so-called Duffing-Van der Pol or Van der Pol-Duffing oscillator) has also been investigated and various bifurcation structures observed (see ref. [9] and references therein).

The particular dynamics of the Van der Pol oscillator has raised the question of the behavior of coupled Van der Pol oscillators or that of systems consisting of Van der Pol oscillator coupled to another type of oscillator.

As concerns coupling between Van der Pol oscillators, some interesting works have been carried out. Rand et al. [10] have investigated various bifurcations of motions of two coupled classical Van der Pol oscillators. They derived criteria or parameters space regions for phase locked periodic motions, phase entrainment and phase drift. The case of two Van der Pol-Duffing oscillators with linear

coupling has also been considered by Polianshenko et al. [11]. They showed that nonisochronism (the dependence of oscillation frequencies on amplitudes) substantially changes the dynamics of the system by generating not only one frequency gap, but also displays two frequencies and chaotic dynamics (the transition to chaos being through period doubling or via type I-intermittency). Additionally, the system exhibits hysteresis between two and one-frequency regimes and between one frequency and suppressed oscillations. The same group also extended their study to include nonlinear coupling terms in ref.[12]. They observed multistability, three frequency oscillations and found the parameters boundaries for chaos using Shilnikov theorem. Transition to hyperchaos has also been reported in coupled Van der Pol-Duffing oscillators [13]. More recently, another nonlinear coupling model has been analyzed in ref.[14]. It was found that the structure of attraction basins is related to the symmetry of the attractors and can be understood using discrete transformations similar to logistic maps.

For the coupling between Van der Pol oscillator and other types of oscillators (e.g. oscillators that cannot sustain their own oscillations), we tackled the problem in ref.[2] by investigating the dynamics of a system consisting of a Van der Pol-Duffing oscillator coupled dissipatively and elastically to a Duffing oscillator. Using the multiple time scales method, we analyzed the oscillatory states both in the resonant and non-resonant cases. Chaos was also found using the Shilnikov theorem.

In this paper, we are dealing with a model consisting of a classical Van der Pol oscillator coupled gyroscopically to a linear oscillator. Three major problems are analyzed. First, the regular dynamics of the system is considered using analytical methods. In the forced case, we find and study the stability of harmonic oscillations using the method of harmonic balance and the Hill determinant procedure. In the autonomous system, the averaging method leads to two types of oscillatory states and indicates the criteria for quenching phenomena in the system. The second problem consists of analyzing the appearance of the chaotic states. Two types of transition indicators are used: the projection of the attractors in the Poincare section onto the system coordinates and the largest Lyapunov exponent, both versus a control parameter (one of the coupling coefficient). It is found that there are domains where chaotic and regular states appear and disappear randomly following very small changes in the coupling coefficient. The synchronization of two or more devices described by our model is also discussed as the third issue of the paper.

The paper is organized as follows. Section 2 presents the model, the resulting harmonic solutions with the stability boundary equation and the oscillatory states in the autonomous system. In section 3, we use the numerical simulation to analyze different types of transition of the system behavior as the coupling coefficient varies. Then, the continuous control strategy is used to synchronize two or more devices in a chaotic state. We conclude in section 4.

II- Model and oscillatory states

II-1- The model:

The model we are dealing with is described by the following set of differential equations

$$\ddot{y} + \varepsilon(y^2 - 1)\dot{y} + y + f\ddot{x} = E\cos(nt) \qquad (1a)$$

$$\ddot{x} + \lambda\dot{x} + x - dy = 0 \qquad (1b)$$

where an overdot denotes time derivative. The Van der Pol oscillator is represented by the variable y while x stands for the linear oscillator. ε and λ are respectively the Van der Pol parameter and the damping coefficient of the linear oscillator. The quantities f and d are the coupling coefficients. E_o and n are the amplitude and frequency of the external excitation while t is the non-dimensional time. We have restricted our analysis to the case where the natural frequencies of both oscillators are identical (internal resonance). This restriction is interesting since it can be shown, using the multiple time scales method [1,2], that in the non internal resonant case, each oscillator tends to behave independently; e.g. they are decoupled from each other. In the paper, d and λ are fixed to d=0.1 and λ=0.1.

The particular type of coupling in eqs.(1) is well known in electromechanical engineering. Indeed the system of eqs.(1) can describe a self-sustained electromechanical transducer consisting of an electrical part (the Van der Pol) and a mechanical part governed by the linear oscillator. The coupling between both parts is realized through the air-gap of a permanent magnet. It creates a Laplace force in the mechanical part and the Lenz electromotive voltage in the electrical part (in this case, y denotes the electric current and x stands for the displacement of a mechanical load). Let us note that the reverse state is also possible where the Van der Pol equation describes the motion of a mechanical system with negative damping while the electrical component is the linear oscillator. Our model can also be used as a vibration controller [16] or in the general field of sensors with self-excited components.

II-2: **Forced harmonic oscillatory states and their stability**:

We seek for harmonic oscillatory solutions of eqs.(1) by using the harmonic balance method. For this purpose, let us express y and x in the form

$$y= a_1\cos(nt)+b_1\sin(nt) \qquad (2a)$$

$$x= a_2\cos(nt)+ b_2\sin(nt) \qquad (2b)$$

Let us set $A_i^2 = a_i^2+b_i^2$ with i=1,2. Inserting eqs. (2) in eqs.(1) and equating the cosine and sine terms separately, we obtain

$$-\varepsilon n a_1 (1 - \frac{A_1^{\,2}}{4}) + b_2 n^2 f = b_1 (1 - n^2) \tag{3a}$$

$$\varepsilon b_1 n (1 - \frac{A_1^{\,2}}{4}) + a_2 n^2 f + E_o = a_1 (1 - n^2) \tag{3b}$$

$$\lambda n a_2 + d b_1 = b_2 (1 - n^2) \tag{3c}$$

$$\lambda n b_2 - d a_1 = -a_2 (1 - n^2) \tag{3d}$$

After some algebraic manipulations, it comes that the amplitude A_i satisfy the following equations

$$A_1^{\,6} + C_1 A_1^{\,4} + C_2 A_1^{\,2} - \frac{E_o^{\,2}}{\mu} = 0 \tag{4a}$$

and

$$A_2^{\,2} = H^2 (1 + S^2) A_1^{\,2} \tag{4b}$$

where

$$S = \frac{1 - n^2}{\lambda n},$$

$$H = \frac{d}{\lambda n (1 + S^2)},$$

$$Q = HSn^2 f - 1 + n^2,$$

$$C_1 = 8\left[\frac{Hfn}{\varepsilon} - 1\right],$$

$$C_2 = 16\left[\left(\frac{Hfn}{\varepsilon} - 1\right)^2 + \frac{Q^2}{\varepsilon^2 n^2}\right]$$

and

$$\mu = \frac{\varepsilon^2 n^2}{16}$$

The oscillatory states (2) are not always realized even if from eq.(4) we obtain values for A_i. Their realization is physically interesting only so long as they are stable. To study the stability, let us consider the following variational equations of (1) around the oscillatory states (2)

$$\ddot{y}_1 + \varepsilon(y^2 - 1)\dot{y}_1 + (1 + 2y\dot{y})y_1 + f\ddot{x}_1 = 0 \qquad (5a)$$

$$\ddot{x}_1 + \lambda\dot{x}_1 + x_1 - dy_1 = 0 \qquad (5b)$$

The oscillatory states are stable if y_1 and x_1 remain bounded as the time grows. The appropriate analytical tool to investigate the stability conditions of the oscillatory states is the Floquet theory [1,5]. With the coupling, it is difficult to develop a Floquet approach for eqs.(5) in the general manner. We restrict our analysis to the case where the fluctuations y_1 and x_1 have the same frequency as the oscillatory states (2). Let us then express y_1 and x_1 in the form

$$y_1 = P_1\cos(nt) + T_1\sin(nt) \qquad (6a)$$

$$x_1 = P_2\cos(nt) + T_2\sin(nt) \qquad (6b)$$

Inserting eqs.(6) into eqs.(5) with y defined by eq.(2a) and making use of the harmonic balance method, we obtain that the condition for non trivial solution for the set (P_1, T_1, P_2, T_2) is given by the equation

$$3A_1^4 + 2C_1A_1^2 + C_2 = 0 \qquad (7)$$

This equation defines the first order stability limit. A_1^2 can be extracted from eq.(7) and then substituted in eq.(3a) to give the boundary of the stability as a function of the parameters f, d, ε ,E_o and n. In fig.1, we have displayed two stability domains in the (f, E_o) plane with n=1 and n=0.8 respectively. In fig.1a, the stability region is the space below the curve while in fig.1b, the oscillatory states are stable inside the enclosed space. Fig.2 presents some response curves as the coupling coefficient f varies. The curves of fig.2 are to be compared with fig.1 to locate the stability limits. For instance, it appears that in fig.2a, the stable amplitudes are on the upper curve and the limit of stability are defined by the lines f=0 and f=fc where fc is the vertical tangency of the response curve. In fig.2b, the stable amplitudes are comprised in the intervals f∈[1.775, 2.140] and f∈[2.375, 2.515].

II-3: **Oscillatory states in the autonomous systems**

We consider here the autonomous model (E_o =0). The appropriate analytical procedure to find the oscillatory solutions is the averaging method [1]. Using this method, we can show that the amplitudes A_1 and A_2 and the phase difference φ between y and x satisfy the following set of first order differential equations

$$\dot{A}_1 = \frac{\varepsilon A_1}{2}\left(1 - \frac{A_1^{\,2}}{4}\right) + \frac{f}{2} A_2 \sin\varphi \qquad (8a)$$

$$\dot{A}_2 = -\frac{1}{2}\lambda A_2 - \frac{dA_1}{2}\sin\varphi \qquad (8b)$$

$$\dot{\varphi} = -\frac{1}{2}\left(\frac{dA_1}{A_2} - \frac{fA_2}{A_1}\right)\cos\varphi \qquad (8c)$$

In the stationary state, eqs.(8) lead to two classes of solutions depending on the values of the parameters of the system. The first class (which can also be derived from eqs.(3)) is given by

$$A_1^{\,2} = 4\left(1 - \frac{fd}{\lambda\varepsilon}\right) \qquad (9a)$$

$$A_2 = \frac{d}{\lambda} A_1 \qquad (9b)$$

with $\varphi = \pm\pi/2$. Eqs.(9) requires the critical condition

$$\varepsilon > fd/\lambda \qquad (9c)$$

For the second class, we have

$$A_1^{\,2} = 4(1 - \lambda/\varepsilon) \qquad (10a)$$

$$A_2 = \frac{d}{f} A_1 \qquad (10b)$$

with $\sin\varphi=\lambda A_2/d A_1$. This second class is valid under the condition

$$\varepsilon>\lambda \qquad (10c)$$

When the conditions (9c) and (10c) are not satisfied, a complete quenching of oscillations takes place. That is $A_1=A_2=0$ (see fig.3). In this state, our model can serve as a vibration absorber of undesirable self-excited vibrations in mechanical systems (the mechanical oscillator having a negative damping of the Van der Pol type). A quenching phenomena of self-excited oscillations has also been reported in ref.[15] for a mechanical Van der Pol oscillator coupled through a damper to a mechanical linear oscillator (the well-known Lanchester damper). But here in our model, the quenching of mechanical self-excited oscillations could be insured by an appropriate choice of physical parameters of an electrical circuit.

III- Chaos and Synchronization

III-1- Windows of chaotic behavior

The aim of this subsection is to analyze some bifurcation structures that can appear in our model as the coupling parameter f varies. Particular attention is paid to transitions from regular to chaotic states. For the purpose, we solve numerically the systems of eqs.(1) along with the variational eqs.(5) using the fourth-order Runge-Kutta algorithm with the time step $h=T/2000$ where $T=2\pi/n$ (n is the frequency of the external excitation). Transitions are observed through the behavior of the projection of the attractors in the Poincare section onto the coordinate y and through

the variation of the Lyapunov exponent. We define the Lyapunov exponent from eqs.(5) as

$$lya = \lim_{\substack{t \to \infty \\ t}} \frac{1}{t} \ln(y_1^2 + \dot{y}_1^2 + x_1^2 + \dot{x}_1^2) \qquad (11)$$

that is the measure of the rate of divergence between initially closed trajectories in the four dimensional phase space (y,dy/dt,x,dx/dt). We have particularly concentrated our analysis to the case where the frequency n of the external excitation is equal to the common natural frequency of oscillators y and x (e.g. n=1). Our various numerical experiments have shown that the "poor" chaotic character of the classical Van der Pol oscillator also manifests itself in our coupled model. Indeed, for small values of ε and E_o , chaos is not found in the system whatever is the coupling coefficient. Therefore, we have taken ε=5 and E_o =0, values for which it is known that chaos is present in the classical Van der Pol oscillator for a small range of the frequency n, typically n $\in$ [2.463, 2.466] (see ref.[6]). Setting d= λ=0.1 and n=1, f is varied in step of 5×10^{-4} from 0 to 5. The scanning has led to the following results. When f is increased from 0, we have a period-1 attractor (harmonic oscillations) until f=2.55. After this value, a secondary Hopf or Neimark bifurcation takes place. A quasiperiodic attractor is born and disappears at f=2.582. From f=2.582 to 4.572, it is found that the system is very sensitive to tiny variations of the coupling coefficient. In fig.4 and fig.5, we present the behavior of the system for f$\in$ [2.8, 3.4]

and f∈ [3.8, 4.65] respectively. Figs.4a and 5a show the variation of the Lyapunov exponent while fig.4b and fig.5b present the corresponding projection of the bifurcation diagrams showing the coordinates y and x of the Poincare section versus f. It is found that the system exhibits a complex bifurcation structure with chaotic points or windows randomly and suddenly alternating with points or windows of regular motion.

Because of the presence of various transition points, we have not analyzed the route to chaos at each point. We have considered the transitions at the borders of the f-intervals of figures 4 and 5. Taking the first border in fig.4, we find that chaos arises after a period-17 attractor. Fig.6 shows a chaotic orbit for f=3.84. From fig.4b and 5b, as well as in fig.7 below, it is observed that the orbits which describe the dynamics of the system in the windows of regular motion also tend to dominate the dynamics of the system in the chaotic seas. Their attracting behavior can be used in the process of chaos control [17].

At f=3.3515, a period-11 orbit takes place and remains until f=3.8240 where it suddenly bifurcates to chaos. From 3.9218 to 4.0845, a period-8 orbit dominates the dynamics of the system with a tiny domain of period-16 orbit. At the upper edge of fig.5, we are in presence of a quasiperiodic sea striped by periodic and chaotic points until f=4.572 where the quasiperiodic sea is destroyed. Then follow period-4→period-2 orbits. But the transition from period-4 to period-2 is abrupt and characterized by the disappearance of two of the four orbits. This phenomenon also appears for the transition from period-8 to period-16 orbits quoted before.

A similar scanning process has been performed to see how the coupling coefficient affects the chaotic domain obtained in ref.[6]. We have thus set n=2.465. Fig.7a presents the variation of the Lyapunov exponent as f varies while fig.7b shows the projection of the y coordinate of the Poincare section. Various small windows of regular motion also randomly alternate with chaotic states. For the windows located near f=0.1 and f=0.3, we have period-13 and period-9 attractors respectively. At the upper edge of these windows of regular motion, it is found that chaos arises following a period doubling. After f=0.56, chaos disappearance follows the route chaos→period-5 attractor.

III-2: **Synchronization**:

Recent years have seen a growing interest in control and synchronization of nonlinear oscillators particularly in their chaotic regimes for potential applications in securing communications (see ref.[17] and references therein). One domain where applications of control and synchronization are needed is the field of electromechanical engineering where, as noted before, devices described the model equations (1) can be found. In fact, even in the telecommunications engineering, emitters and receivers are of the electromechanical type (for instance loudspeakers and microphones).

In our model, both the autonomous and the non-autonomous regimes are of interest and two or more devices can be considered. In the autonomous regime, the synchronization aims to phase locked trajectories of devices in phase since when

they are started with different initial conditions, their trajectories tend to a common limit cycle, but with different phases. This problem has been considered recently by Leung [18] for the synchronization of classical autonomous Van der Pol oscillators. In the non-autonomous case, the synchronization process is interesting in the chaotic regimes. In case of a series of devices, the continuous control strategy [17] can be implemented in two ways. In the first way, the master device controls directly the motion of the enslaved devices. The second way consists of a series of cascading control. The master controls the first slave which in its turn controls the second slave, etc. We assume that the slave devices are set in motion at the same time with identical initial conditions and that the control is launched at the same time in the lattice. It is found, as one could presume, that the time to achieve the total synchronization over the entire lattice of devices is shorter in the first way than in the second way. Fig.8 shows the chaotic synchronization transient dynamics in the case of three devices: y, z and v are respectively the Van der Pol components of the master, first slave and second slave (controlled by the first slave). If the second slave was directly coupled to the master, then its synchronization transient dynamics would have been identical to fig.8a.

IV- Conclusion

In this paper, we have considered the dynamics of a system consisting of a Van der Pol oscillator coupled to a linear oscillator. The coupling, of gyroscopic type, can be encountered in various electromechanical devices. In the forced regime, the

amplitude and the stability boundaries of the harmonic behavior have been obtained. In the autonomous system, two types of oscillatory motions are found and can be totally quenched when some critical relations between the physical parameters of the model are satisfied.

A direct numerical simulation of the model equations has complemented the analytical results. It appears that for some particular set of parameters, windows of chaos randomly alternate with windows of regular (period-m) orbits. Two main transitions to chaos have been observed: from period-m (e.g.;m=5.8,11, 17) orbits to chaos and from period-doubling to chaos. We have finally given some indications on the importance of synchronizing some types of motions with extension to a lattice of devices described by our model.

In the paper, we have restricted our analytical investigations to the study of harmonic oscillatory states. It would be interesting to consider the case of sup- and sub- harmonic entrainments as well as the conditions for the system to exhibit almost or quasiperiodic oscillations. Moreover, a generalization of our model to include other nonlinear terms (e.g., a Van der Pol-Duffing oscillator with soft or hard nonlinearity coupled gyroscopically to a linear oscillator) and the experimental study of a prototype of our model are under investigation.

Acknowledgements

This work was done within the framework of the Associateship Scheme of the Abdus Salam International Centre for Theoretical Physics, Trieste, Italy. Financial support from the Swedish Agency for Research Cooperation with Developing Countries is acknowledged.

References

[1] A.H. Nayfeh and D.T. Mook , ***Nonlinear Oscillations*** (Wiley, New York, 1979).

[2] P.Woafo, J. C. Chedjou and H.B. Fotsin, Phys.Rev.E**54**, 5929 (1996)

[3] P.Woafo, H.B.Fotsin and J.C.Chedjou, Physica Scripta **57**, 195 (1998).

[4] B. Van der Pol, Philos. Mag.**43**, 700 (1922);**7-2**, 978 (1926);
7-3, 65 (1927); Proc. IRE **22**, 1051 (1934).

[5] C. Hayashi, ***Nonlinear Oscillations in Physical Systems*** (McGraw Hill, New York, 1964), Chap.12.

[6] U. Parlitz and W. Lauterborn, Phys.Rev.A**36**, 1428 (1987).

[7] J. Guckenheimer and P.J. Holmes, ***Nonlinear Oscillations, Dynamical Systems, and Bifurcations of Vector Fields*** (Springer-Verlag, Berlin 1984).

[8] W.H. Steeb and A. Kunick, Int. J. Non-Lin. Mech.**22**, 349 (1987).

[9] A. Venkatesan and M.Lakshmanan, Phys. Rev.E**56**, 6321 (1997).

[10] R.H. Rand and P.J. Holmes, Int. J. Non-Lin. Mech. **15**, 387 (1980);
- D.W. Storti and R.H. Rand, idem **17**, 143 (1982);
- T. Chakraborty and R.H. Rand, idem **23**, 369 (1988).

[11] M. Polianshenko, S. R. McKay and C.W. Smith, Phys. Rev. A**44**, 3452 (1991);
-Idem, Phys.Rev.A**43**, 5638 (1991).

[12] M. Polianshenko and S.R. McKay, Phys.Rev.A**46**, 5271 (1992).

[13] T. Kapitaniak and W.H. Steeb, Phys. Lett.A**152**, 33 (1991).

[14] I. Pastor-Diaz and S.A. Lopez-Fraguas, Phys. Rev.E**52**, 1480 (1995).

[15] K.R. Asfar, Trans. ASME J.Vib. Acoustics, Stress, and Reliability in Design **111**, 130 (1989).

[16] Y.Okada, K. Matsuda and H. Hashitani, J. Vib.Acoustics **117**, 411 (1995).

[17] T. Kapitaniak, ***Controlling Chaos*** (Academic Press, London, 1996);
M. Lakshmanan and K. Murali, ***Chaos in Nonlinear Oscillators, Controlling and Synchronization*** (World Scientific, Singapore, 1996).

[18] H.K. Leung, Phys. Rev. E**58**, 5704 (1998).

Figure Captions

Fig.1 a- Stability domain in the (f, E_o) plane for n=1 and ε=0.3 (below the curve).

b- Stability domain in the (f, E_o) plane for n=0.8 and ε=0.3 (enclosed space).

Fig.2: a- Response curve $A_1^2(f)$ for n=1, ε=0.3 and E_o = 0.1 (crosses) and E_o =0.2 (squares).

b- Response curve $A_1^2(f)$ for n=0.8, ε=0.3 and E_o = 0.1.

Fig.3: a- Oscillatory state in the autonomous system for ε=0.15 (ε>λ) and f=0.2.

b- Quenching phenomena for ε=0.05 (ε<λ) and f=0.2.

Fig.4: a- Lyapunov exponent versus f for f ∈ [2.8,3.4], n=1,ε= E_o =5.

b- Bifurcation diagram showing the coordinate y of the Poincare section versus f for f ∈ [2.8,3.4], n=1,ε= E_o =5.

Fig.5: a- : a- Lyapunov exponent versus f for f ∈ [3.8,4.65], n=1,ε= E_o =5.

b- Bifurcation diagram showing the coordinate x of the Poincare section versus f for f ∈ [3.8,4.65], n=1,ε= E_o =5.

Fig.6: A chaotic orbit for ε= E_o =5 and f=3.84 (lya=0.014).

Fig.7: a-Lyapunov exponent versus f for n=2.465, ε= E_o =5.

b- Bifurcation diagram showing the coordinate y of the Poincare section versus f for n=2.465, ε= E_o =5.

Fig.8: a-Chaotic synchronization transient dynamics y-z for n=2.465, ε= E_o =5.

b- Chaotic synchronization transient dynamics y-v for n=2.465,ε= E_o =5 (v is controlled by z).

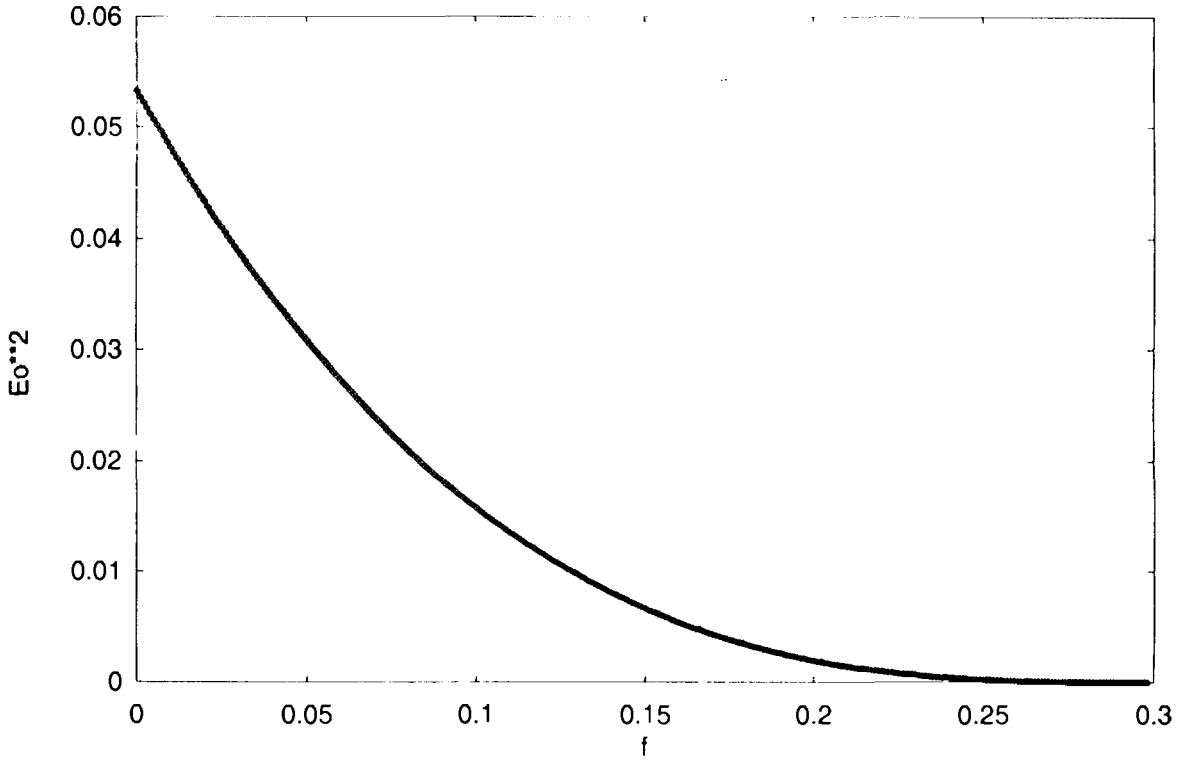
0.06
0.05
0.04
0.03
0.02
0.01
0
Eo**2
0
0.05
0.1
0.15
0.2
0.25
0.3
f

Fig.1a

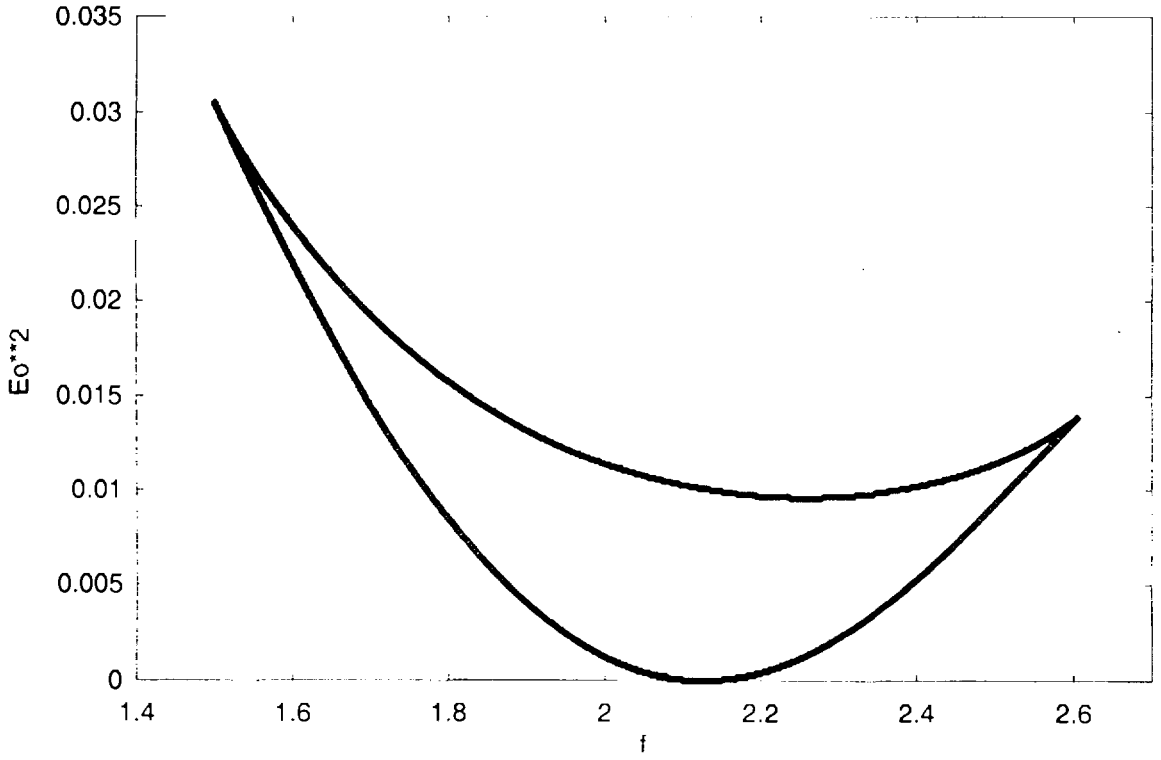
0.035
0.03
0.025
0.02
0.015
0.01
0.005
0
Eo**2
1.4
1.6
1.8
2
2.2
2.4
2.6
f

Fig.1b

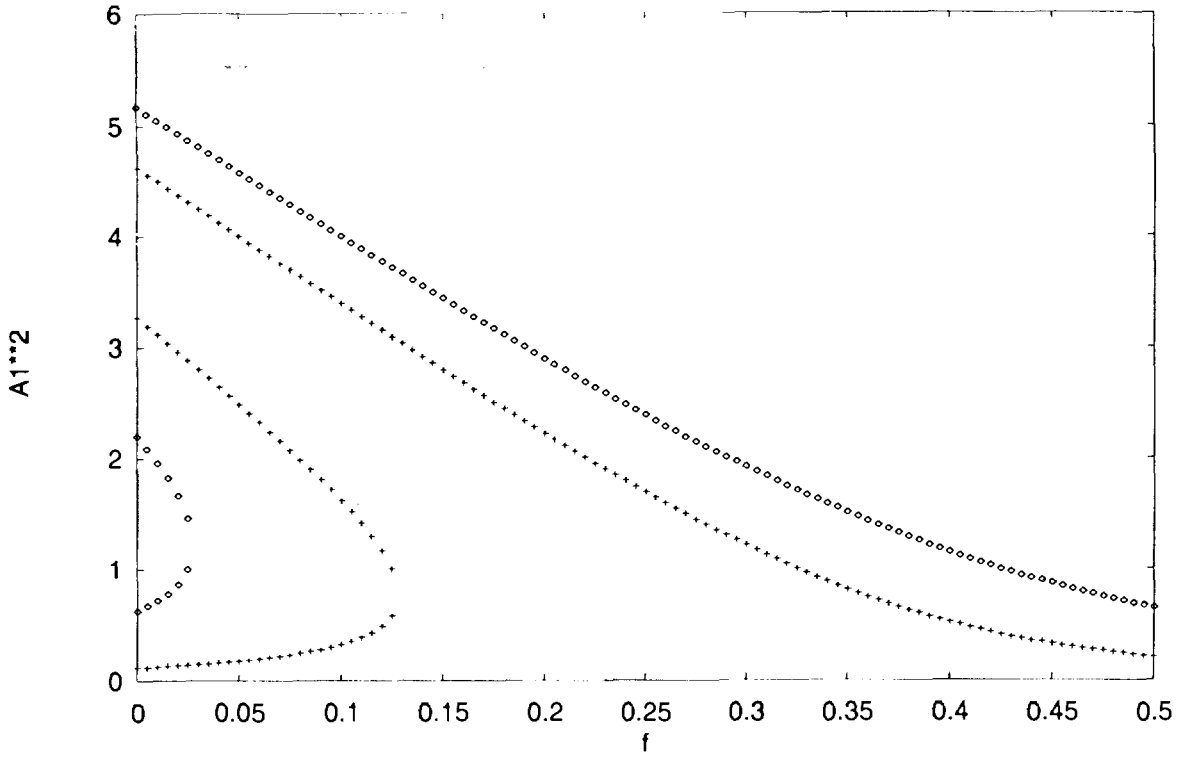
A1**2
f
0
1
2
3
4
5
6
0
0.05
0.1
0.15
0.2
0.25
0.3
0.35
0.4
0.45
0.5

Fig.2a

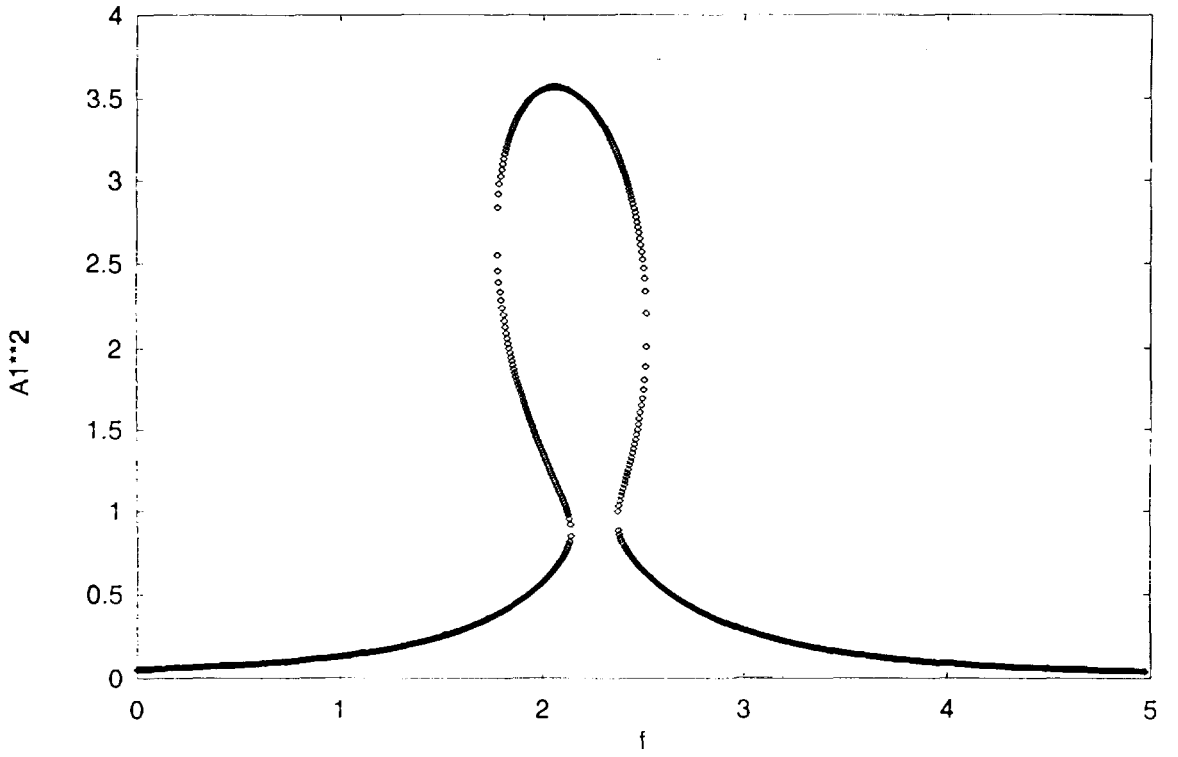
A1**2
f
0
0.5
1
1.5
2
2.5
3
3.5
4
0
1
2
3
4
5

Fig.2b

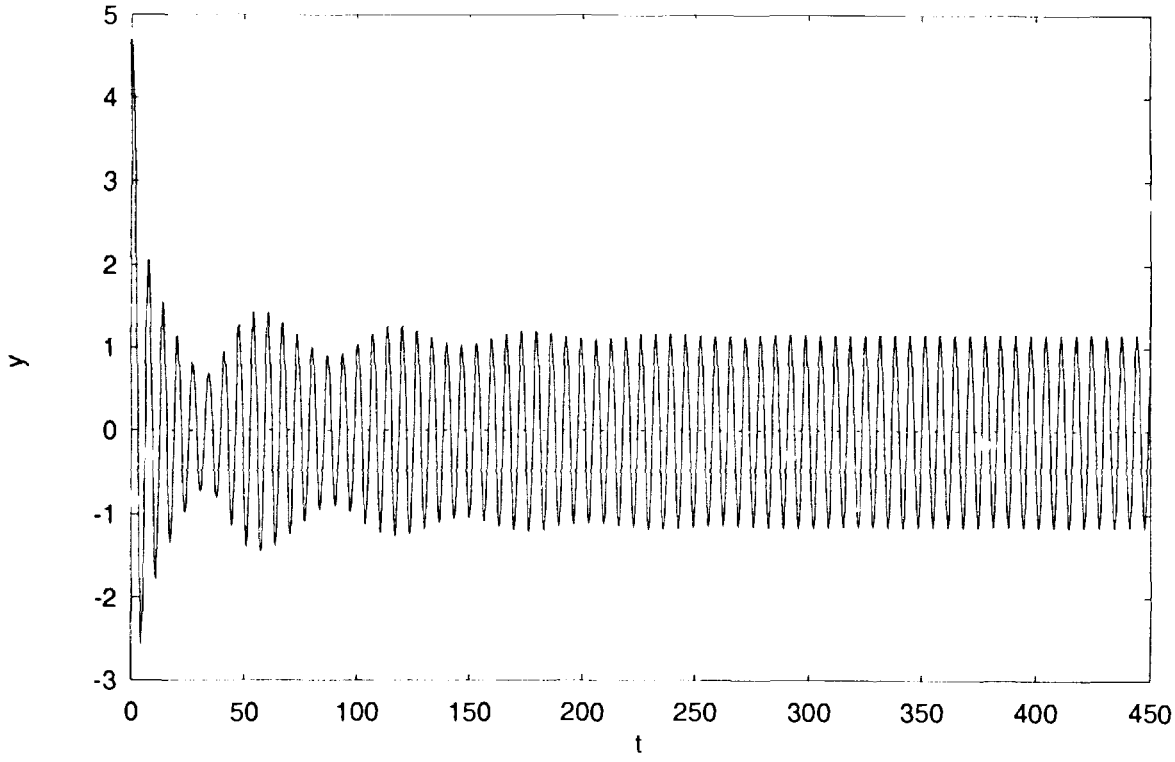
5
4
3
2
1
0
-1
-2
-3
y
0
50
100
150
200
250
300
350
400
450
t

Fig.3a

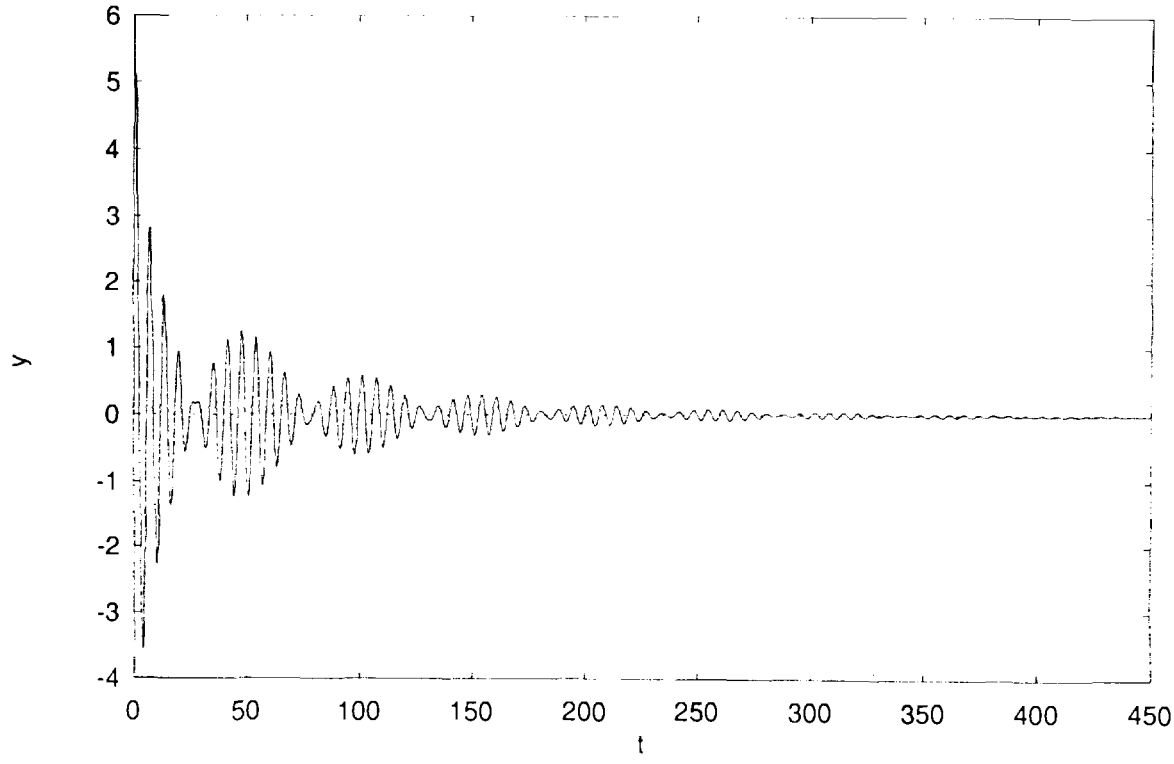
6
5
4
3
2
1
0
-1
-2
-3
-4
y
0
50
100
150
200
250
300
350
400
450
t

Fig.3b

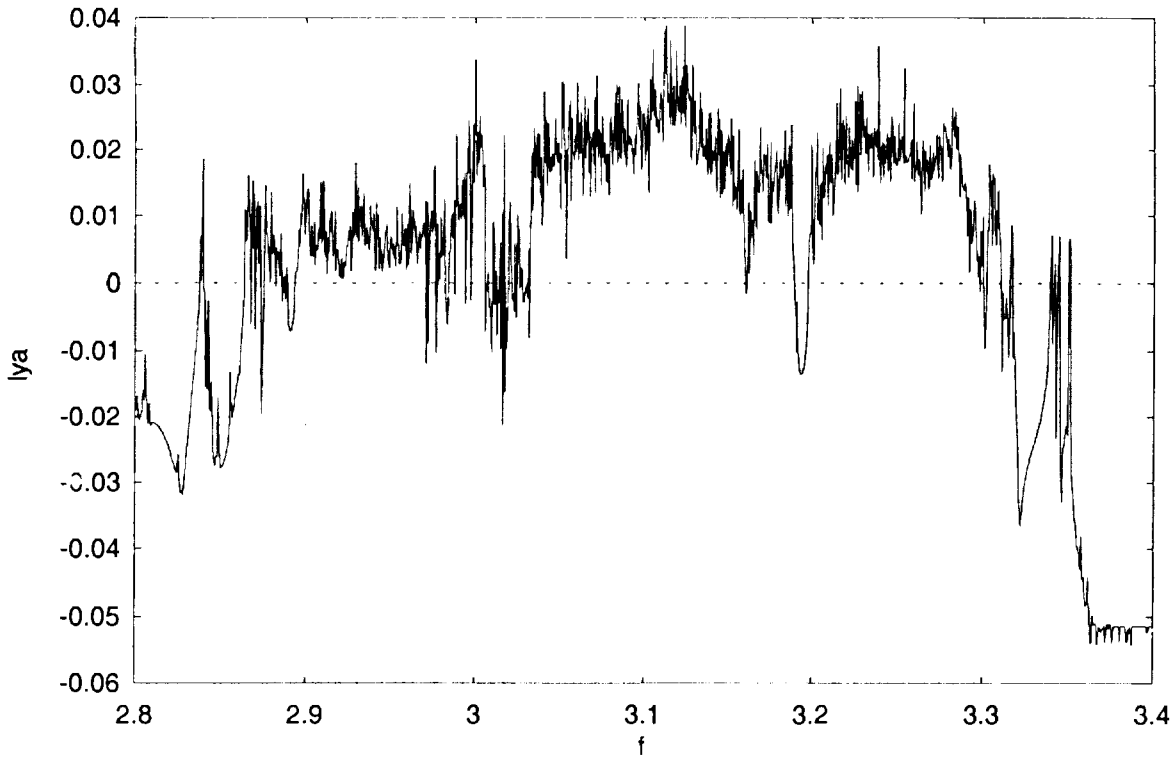
0.04
0.03
0.02
0.01
0
-0.01
-0.02
-0.03
-0.04
-0.05
-0.06
lya
2.8
2.9
3
3.1
3.2
3.3
3.4
f

Fig.4a

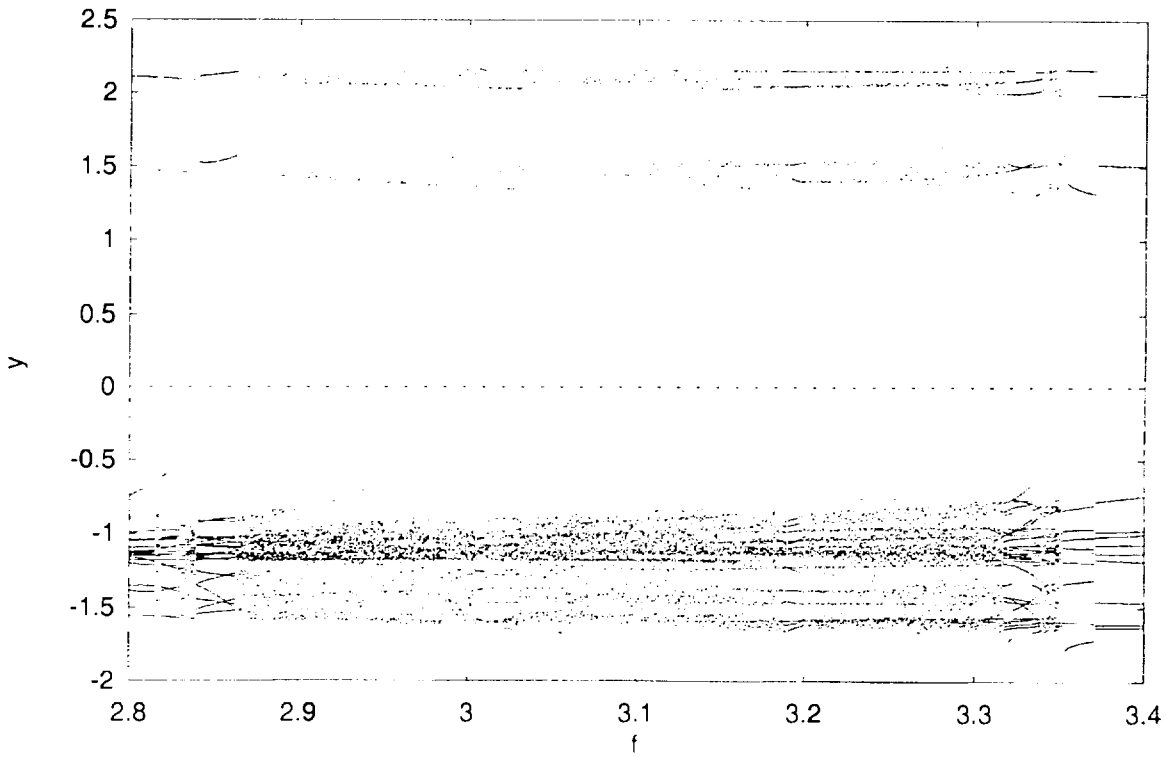
2.5
2
1.5
1
0.5
0
-0.5
-1
-1.5
-2
y
2.8
2.9
3
3.1
3.2
3.3
3.4
f

Fig.4b

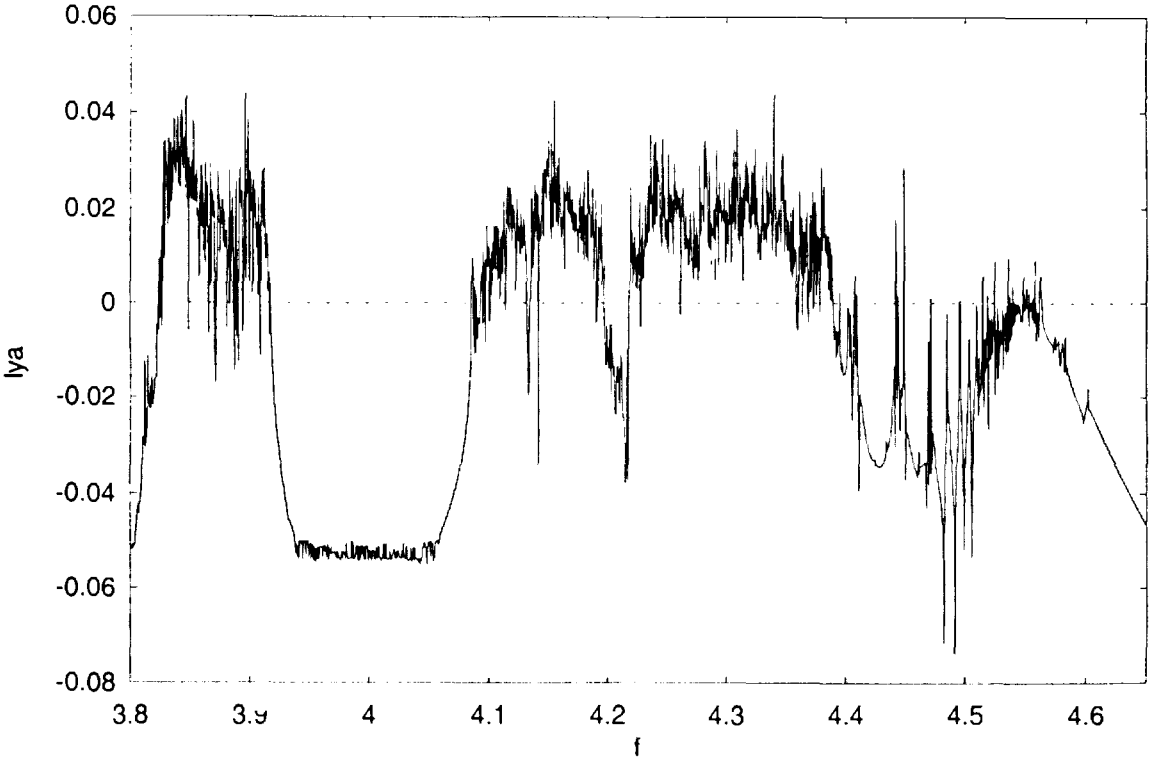
0.06
0.04
0.02
0
-0.02
-0.04
-0.06
-0.08
lya
3.8
3.9
4
4.1
4.2
4.3
4.4
4.5
4.6
f

Fig.5a

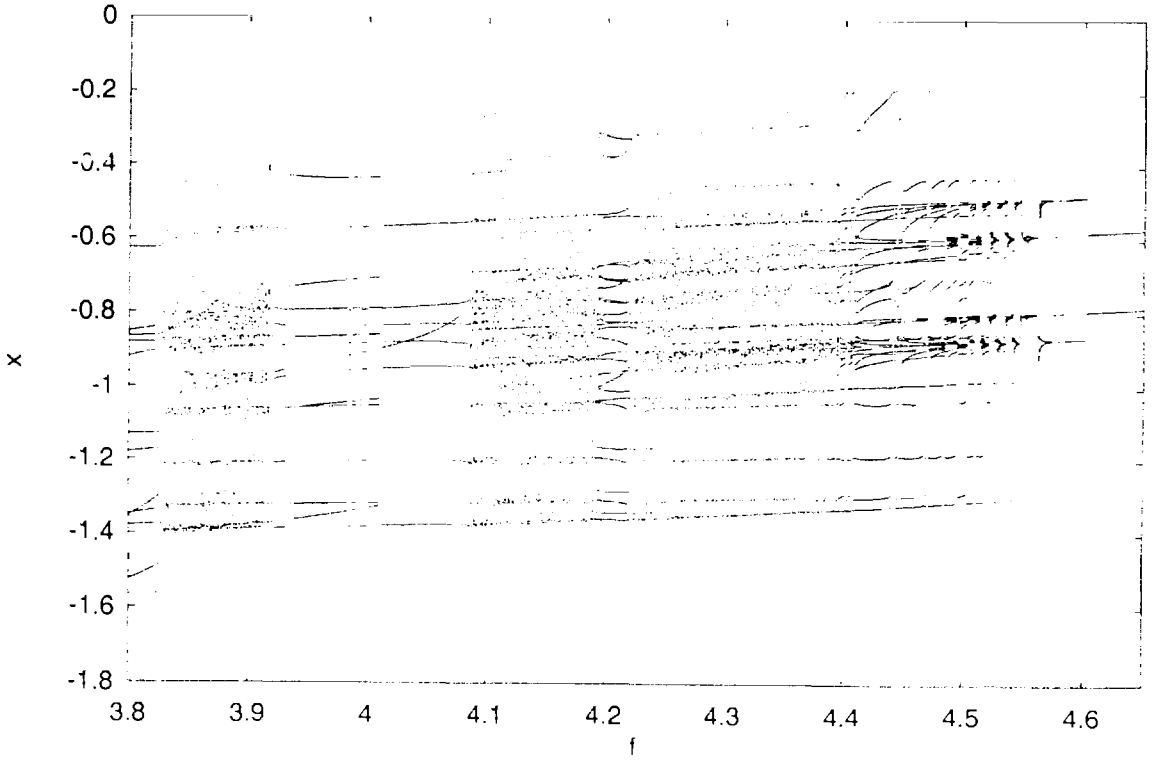
0
-0.2
-0.4
-0.6
-0.8
-1
-1.2
-1.4
-1.6
-1.8
x
3.8
3.9
4
4.1
4.2
4.3
4.4
4.5
4.6
f

Fig.5b

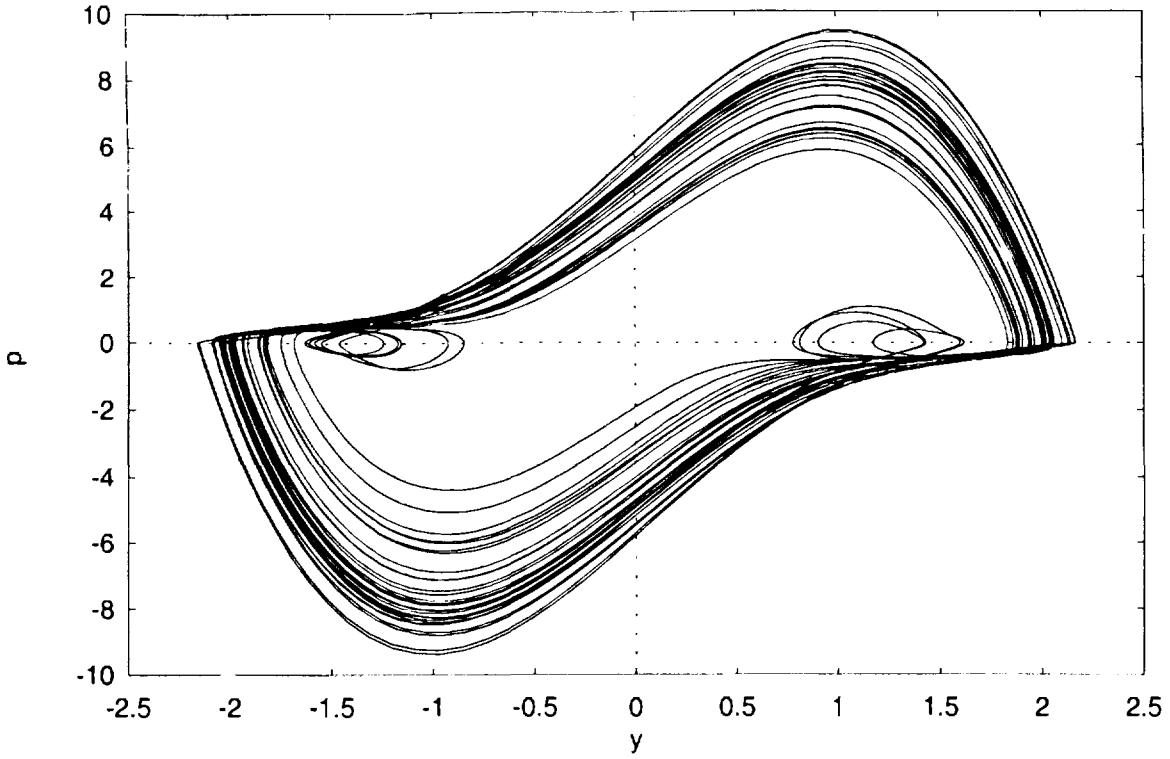

Fig.6

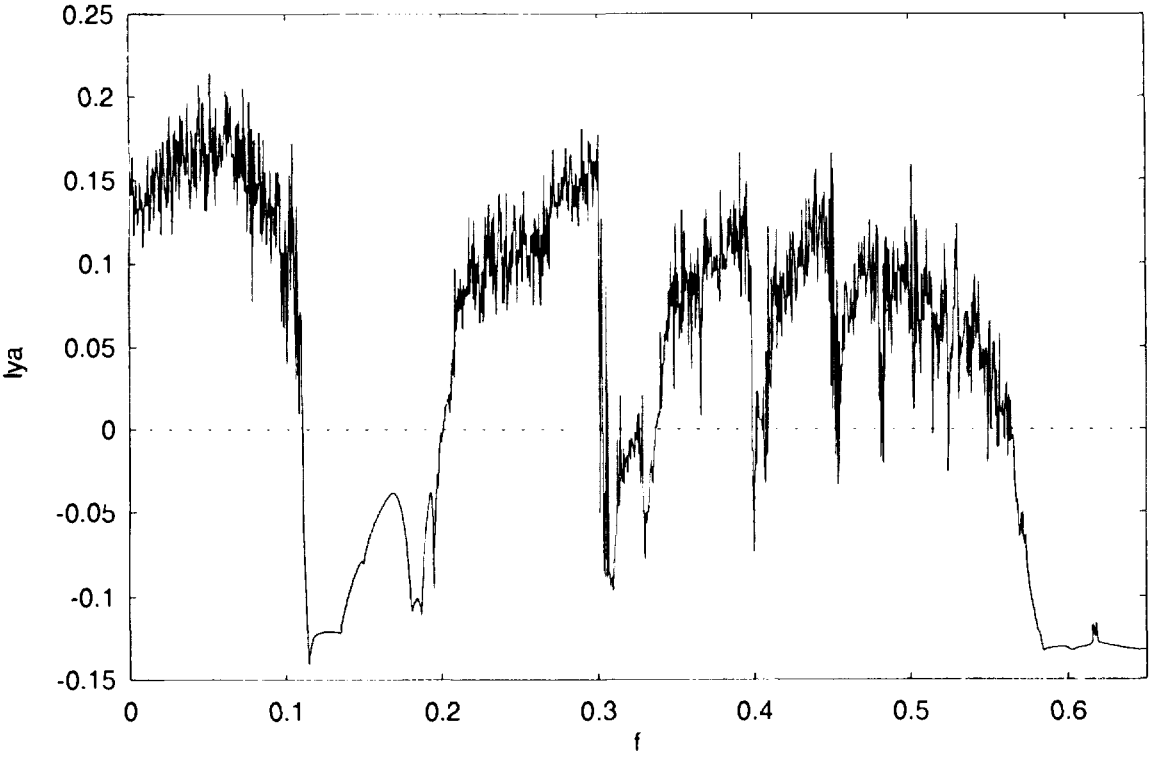
0.25
0.2
0.15
0.1
0.05
0
-0.05
-0.1
-0.15
lya
0
0.1
0.2
0.3
0.4
0.5
0.6
f

Fig.7a

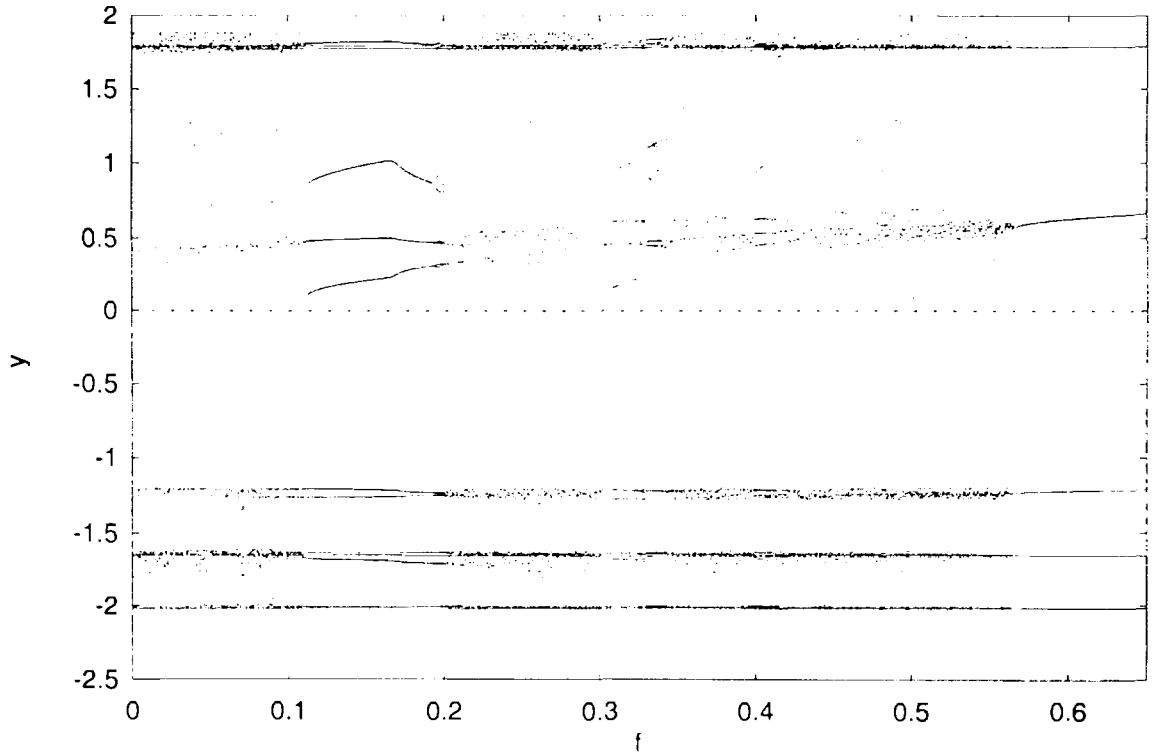
2
1.5
1
0.5
0
-0.5
-1
-1.5
-2
-2.5
y
0
0.1
0.2
0.3
0.4
0.5
0.6
f

Fig.7b

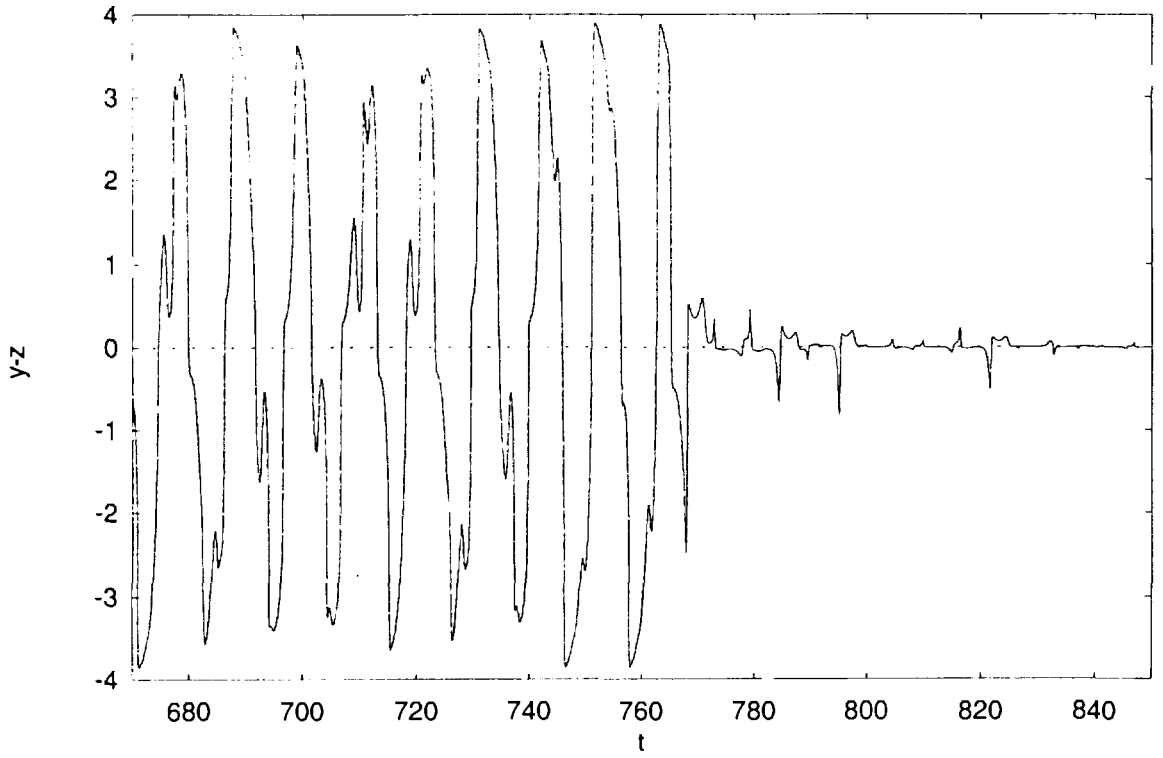
y-z
4
3
2
1
0
-1
-2
-3
-4
680
700
720
740
760
780
800
820
840
t

Fig.8a

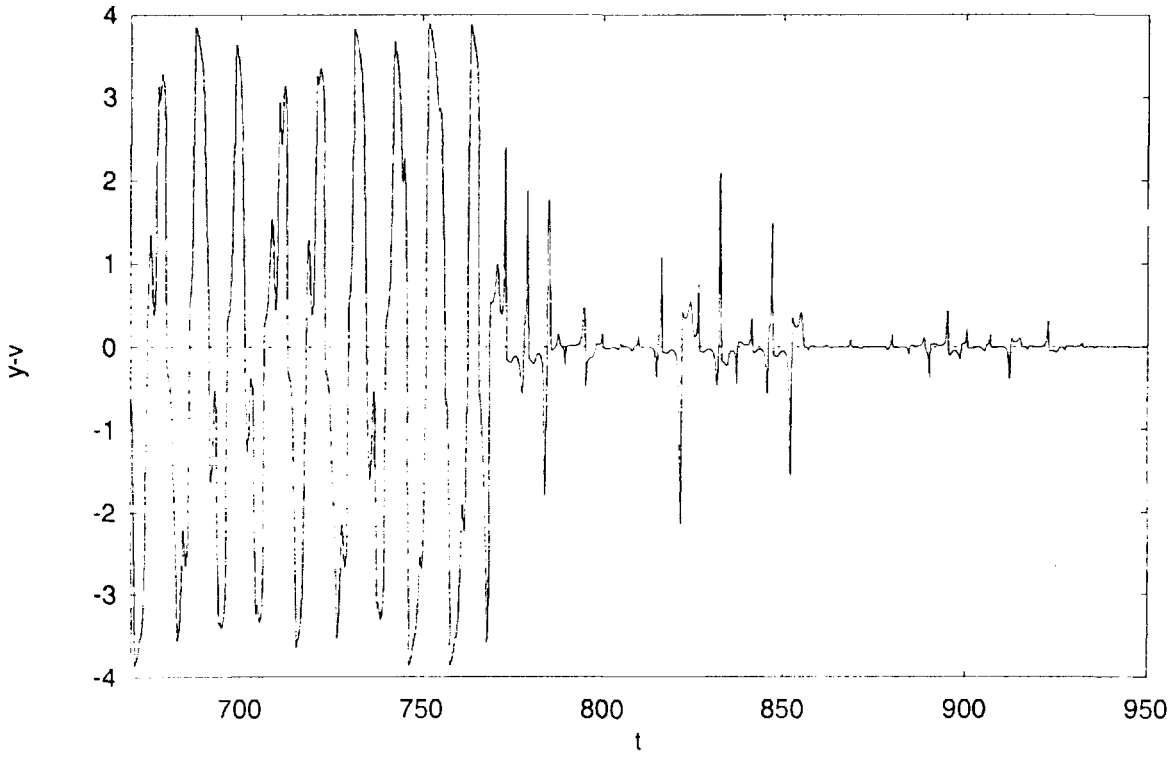
y-v
4
3
2
1
0
-1
-2
-3
-4
700
750
800
850
900
950
t

Fig.8b